Authors' reply to Reviewer's comment 1

January 21, 2019

In the paper, Stokes' equation was solved for a flowline model with only one horizontal dimension and with the boundary conditions of a frozen glacier: no inflow at the upstream boundary, $u = 0$, and no slip at the basal boundary, $u = w = 0$. The failure region and the cliff calving law were determined for this setup.
The anonymous reviewer pointed out that in most scenarios where cliff calving might happen, the glacier will probably be sliding and experiencing lateral drag, and asked what this means for the derived cliff calving law and whether it could be applied in these cases.
We will investigate these two questions here and find that the derived cliff calving rate can serve as a lower bound for cases with sliding and lateral drag.

1 Sliding glaciers

Let's first consider sliding with a constant velocity v (i.e. vanishing strain rate). Then the upstream boundary condition sees an influx with velocity v, so $u = v$. The basal boundary conditions become $u = v$, $w = 0$. Solving the Stokes' equations with these boundary conditions numerically with FeniCS gives the exact same stress fields as in the frozen case (with deviations on the order of magnitude of numerical error, see fig. 1) and the velocity field is simply shifted by the sliding velocity v. This is not surprising: A simple Galilei transformation takes this sliding glacier back to the frozen glacier previously considered without changing any of the physics.
Thus, the assumption made in the paper can be generalized: The cliff calving law derived is valid for glaciers sliding with a constant velocity v with a vanishing strain rate in the last few kilometers before the terminus.
In general, sliding velocities increase towards the glacier terminus. The steepest possible veloctiy gradient can be obtained with a free-slip basal boundary condition: we assume no influx at the upstream boundary, $u = 0$, and at the bed we assume free slip in the horizontal direction, which only leaves a boundary condition for the vertical velocity, $w = 0$. The basal velocity is zero at the upstream boundary and takes its maximum at the calving front. Due to this velocity gradient, the maximum shear stress is large throughout the whole numerical domain (see fig. 2). For increasing ice thickness it becomes difficult to define a meaningful failure region, because the critical shear stress is exceeded in the whole numerical domain - one must assume that the whole numerical domain will fail.
Thus, in the case of a non-vanishing velocity gradient, the failure region is larger than in the case of a vanishing velocity gradient. Hence, the derived cliff calving rate can serve as a lower bound for this kind of calving fronts. In case the sliding velocity was decreasing towards the calving front, the failure region and hence the calving rate would be smaller, but that is very

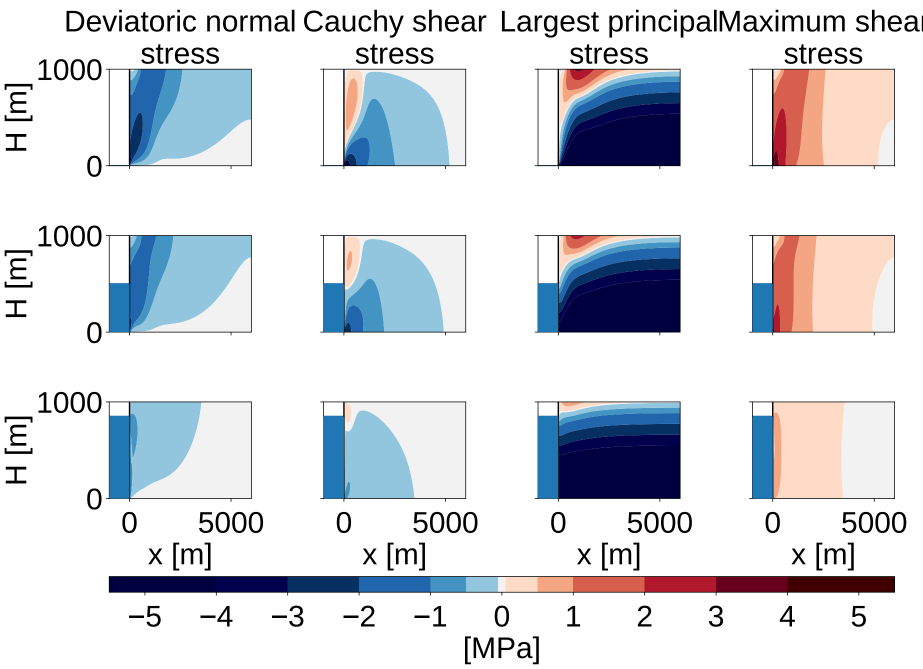

Figure 1: Stresses for the no-slip case, equivalent to sliding with a constant velocity v with vanishing velocity gradient, for three different relative water depths, $w = [0, 0.5, 0.85]$.

unlikely to occur.
To summarize: The derived cliff calving law is valid for glaciers that are frozen to the bed or sliding with a constant velocity and vanishing velocity gradient. It serves as a lower bound on the calving rate for glaciers in which velocities increase towards the calving front.

2 Lateral drag

In order to investigate how lateral drag influences cliff calving, we will assume ice flow in a channel with a flowline in the x-direction. Ice is assumed to flow only in the x-direction with a flow maximum in the middle of the channel (see fig. 3). Since deviatoric stresses are connected to the strain rate, $\tau_{ij} = B\dot{\epsilon}_e\dot{\epsilon}_{ij}$, and the strain rate is given by the velocity gradients, $\dot{\epsilon}_{ij} = \frac{1}{2}\left(\partial_i u_j + \partial_i u_j\right)$, we get an additional deviatoric shear stress in the x-y-plane, τ_{xy}. The other stress components in y vanish, $\tau_{yz} = \tau_{yy} = 0$, because the respective velocity gradients vanish. The Cauchy stress tensor becomes

$$\sigma = \begin{pmatrix} P + \tau_{xx} & \tau_{xy} & \tau_{xz} \\ \tau_{xy} & P & 0 \\ \tau_{xz} & 0 & P - \tau_{xx} \end{pmatrix} \tag{1}$$

The principal stresses σ_i are defined as eigenvalues of σ, and the maximum shear stress τ_{max} as the the difference between the maximum and minimum principal stress. In 2D, there is a simple analytical formula for τ_{max}. In 3D, there is no simple analytical formula for the eigenvalues of a matrix and therefore it is not feasible to get an analytical estimate on whether

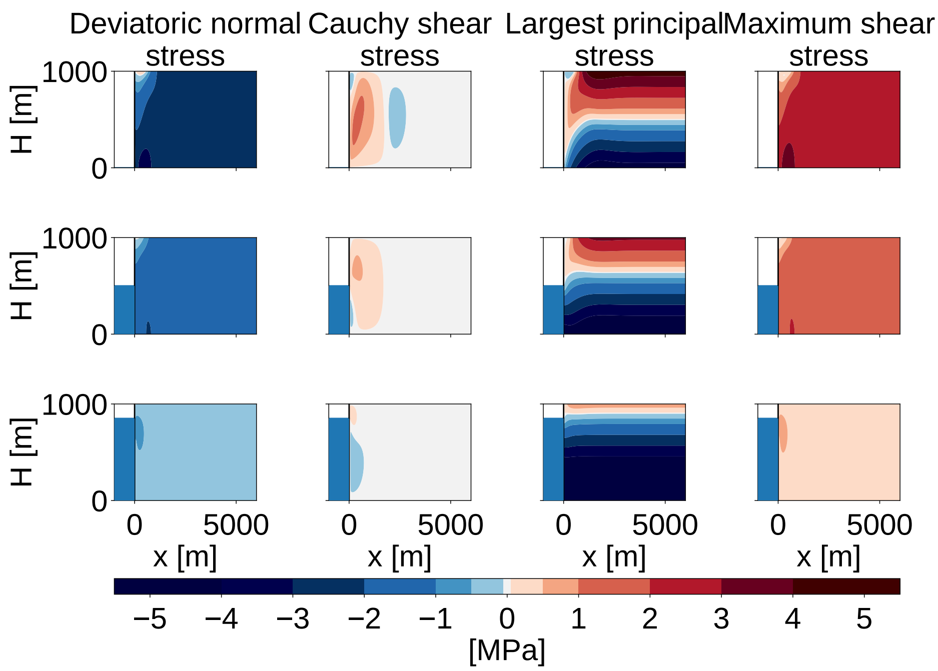

Figure 2: Stresses for the free-slip case for three different relative water depths, $w = [0, 0.5, 0.85]$.

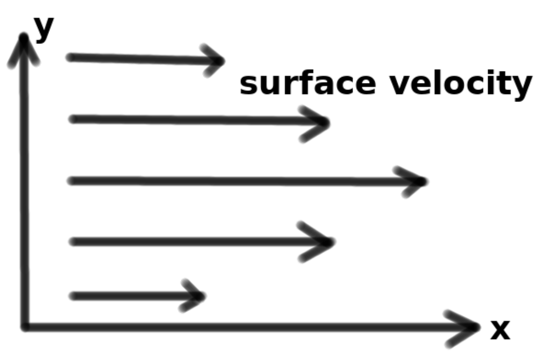

Figure 3: Sketch of the velocity field for ice flow expiriencing lateral drag.

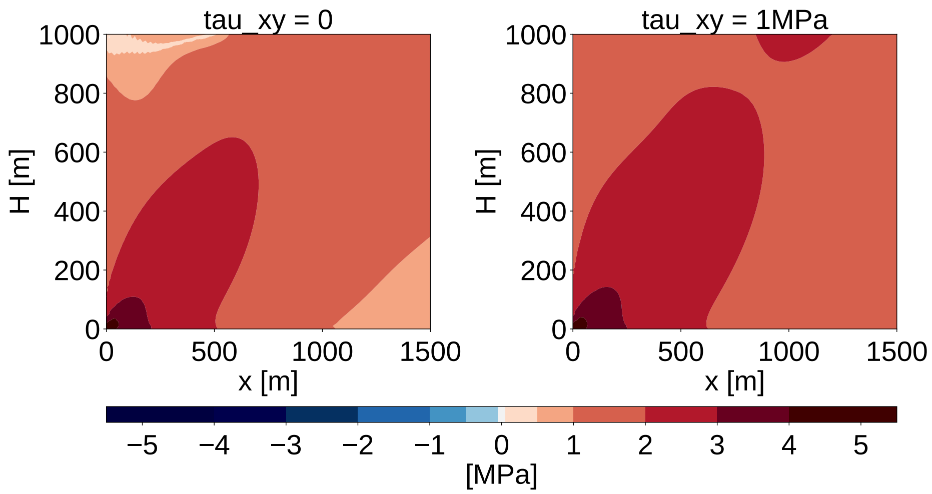

Figure 4: Maximum shear stress τ_{max} in the vicinity of the calving front in the case without lateral drag (left) and with a constant lateral drag of $\tau_{xy} = 1\,\mathrm{MPa}$ (right).

the introduction of non-zero τ_{xy} makes τ_{max} smaller or larger.
Assuming $P(x, z)$, $\tau_{xx}(x, z)$ and $\tau_{xz}(x, z)$ as given by the FeniCS simulation with a constant $\tau_{xy} = 1\,\mathrm{MPa}$, we calculate the principal stresses and the maximum shear stress numerically. This shows that τ_{max} increases with increasing absolute value of τ_{xy} (see fig. 4).
Hence, lateral shear increases the maximum shear, therefore increasing the size of the failure region and the cliff calving rate. The derived cliff calving rate can serve as a lower bound if lateral drag is present.